Applied Microbiology and Biotechnology (2023) 107:623–638
https://doi.org/10.1007/s00253-022-12327-w

BIOTECHNOLOGICAL PRODUCTS AND PROCESS ENGINEERING

Biogenic nanosilver-fabricated endotracheal tube to prevent microbial colonization in a veterinary hospital

Sakkarin Lethongkam[1,2,3] · Jutapoln Sunghan[4] · Chalika Wangdee[5] · Sumit Durongphongtorn[5] · Ratchaneewan Siri[6] · Suttiwan Wunnoo[3] · Supakit Paosen[1,2,3] · Supayang P. Voravuthikunchai[1,2,3] · Krittee Dejyong[4] · Chalongrat Daengngam[6]

Received: 9 May 2022 / Revised: 29 October 2022 / Accepted: 6 December 2022 / Published online: 23 December 2022

Abstract

COVID-19 patients have often required prolonged endotracheal intubation, increasing the risk of developing ventilator-associated pneumonia (VAP). A preventive strategy is proposed based on an endotracheal tube (ETT) modified by the in situ deposition of eucalyptus-mediated synthesized silver nanoparticles (AgNPs). The surfaces of the modified ETT were embedded with AgNPs of approximately 28 nm and presented a nanoscale roughness. Energy dispersive X-ray spectroscopy confirmed the presence of silver on and inside the coated ETT, which exhibited excellent antimicrobial activity against Gram-positive and Gram-negative bacteria, and fungi, including multidrug-resistant clinical isolates. Inhibition of planktonic growth and microbial adhesion ranged from 99 to 99.999% without cytotoxic effects on mammalian cells. Kinetic studies showed that microbial adhesion to the coated surface was inhibited within 2 h. Cell viability in biofilms supplemented with human tracheal mucus was reduced by up to 95%. In a porcine VAP model, the AgNPs-coated ETT prevented adhesion of *Pseudomonas aeruginosa* and completely inhibited bacterial invasion of lung tissue. The potential antimicrobial efficacy and safety of the coated ETT were established in a randomized control trial involving 47 veterinary patients. The microbial burden was significantly lower on the surface of the AgNPs-coated ETT than on the uncoated ETT ($p < 0.05$).

Key points

- *Endotracheal tube surfaces were modified by coating with green-synthesized AgNPs*
- *P. aeruginosa burden of endotracheal tube and lung was reduced in a porcine model*
- *Effective antimicrobial activity and safety was demonstrated in a clinical trial*

Keywords Ventilator-associated pneumonia · Endotracheal tube · Silver nanoparticles · Biofilms · Animal models · COVID-19

✉ Krittee Dejyong
krittee.d@psu.ac.th

✉ Chalongrat Daengngam
chalongrat.d@psu.ac.th

[1] Division of Biological Science, Faculty of Science, Prince of Songkla University, Hat Yai, Songkhla 90110, Thailand

[2] Natural Product Research Center of Excellence, Faculty of Science, Prince of Songkla University, Hat Yai, Songkhla 90110, Thailand

[3] Center of Antimicrobial Biomaterial Innovation-Southeast Asia, Prince of Songkla University, Hat Yai, Songkhla 90110, Thailand

[4] Faculty of Veterinary Science, Prince of Songkla University, Hat Yai, Songkhla 90110, Thailand

[5] Department of Veterinary Surgery, Faculty of Veterinary Science, Chulalongkorn University, Henri-dunant, Bangkok 10330, Thailand

[6] Division of Physical Science, Faculty of Science, Prince of Songkla University, Hat Yai, Songkhla 90110, Thailand

Introduction

Ventilator-associated pneumonia (VAP) is the most common hospital-acquired infection in patients receiving mechanical ventilation. It remains a serious complication, especially in critically ill patients, as pneumonia increases the risk of death. VAP is associated with prolonged hospitalization, increased health care costs, and high mortality. During the COVID-19 pandemic, a large number of infected patients have needed endotracheal intubation and mechanical ventilation because of respiratory failure (Ippolito et al. 2021; Wu and McGoogan 2020). These patients have often required prolonged periods of intubation, which has increased the risk of developing VAP (Chang et al. 2021; Giacobbe et al. 2021).

An initial and important step in VAP pathogenesis is microbial adhesion to the surface of the endotracheal tube (ETT). Adhered microorganisms can colonize the ETT surface within a few hours of intubation (Gorman et al. 1993), and the formation of a biofilm matrix follows. Biofilm can then become dislodged from the ETT surface and migrate to lung tissues, resulting in VAP (Adair et al. 1999; Feldman et al. 1999). *Acinetobacter baumannii*, *Pseudomonas aeruginosa*, and *Staphylococcus aureus* are among the leading causes of VAP, and are often resistant to most available antibiotics (Bonell et al. 2018). Therefore, the prevention of bacterial adhesion and biofilm formation has frequently been the aim of strategies to counter VAP pathogenesis. The surfaces of ETT can be modified with a biocidal coating that can be based on antibiotics, disinfectants, antimicrobial peptides, or metal coatings. The antimicrobial mechanisms of these active coatings may rely on the release of antibacterial agents or on physical disruption caused when pathogens come into contact with the ETT surface (Mas-Moruno et al. 2019).

Although several attempts at coating ETT surfaces have shown good antimicrobial activity in vitro, the efficacy of a coated ETT has rarely been reported for an animal model that closely reflects the primary pathogenic mechanisms of VAP in humans. A study that used ventilated dogs challenged with oral administration of *P. aeruginosa* found that the *P. aeruginosa* burden was significantly lower on the surfaces of a silver-coated ETT than an uncoated ETT, and that the improvement extended to lung tissue (Olson et al. 2002). A silver-coated ETT was also associated with delayed VAP onset in intubated patients (Kollef et al. 2008). However, ETT modified in this way have not gained widespread approval in clinical settings because the cost is about 50 times more than a conventional, unmodified ETT.

Silver nanoparticles (AgNPs) are attracting interest as antimicrobial agents because the small size of the molecule (1 to 100 nm) increases the surface area available for close interaction with bacterial cells. We previously developed a green-synthesized AgNPs-coated ETT using a layer-by-layer self-assembly method (Daengngam et al. 2019) and an ETT coated using a dipping method with a polyamide/silver nanoparticle composite (Lethongkam et al. 2020). These approaches provided good, broad-spectrum antimicrobial activity with no cytotoxic effects on human lung epithelial cells. However, in clinical use, ETT are connected to mechanical ventilators to create a respiratory cycle for intubated patients, and the coatings required polymers to stabilize and retain the AgNPs on the surface of the ETT. The presence of polymers may reduce the lumen of the ETT and decrease the airflow, particularly in a small ETT. Moreover, long-term use can degrade the polymer layers and reduce the antimicrobial efficacy of coatings (Roosjen et al. 2006).

In this study, a novel AgNPs-coated ETT was produced in a green synthesis by directly infiltrating AgNPs into the ETT surface. The coating method did not require any intermediate polymer to capture AgNPs on the ETT surface. In vitro experiments in simulated biological conditions of VAP demonstrated the excellent antimicrobial effectiveness of the AgNPs-coated ETT. In a preclinical study of a porcine VAP model, the coating prevented *P. aeruginosa* colonization of ETT surfaces and lung tissues. In a randomized controlled trial in a veterinary hospital, the bacterial burden on ETT surfaces was significantly reduced.

Materials and methods

Materials

Silver nitrate (99.9999%) was purchased from Sigma-Aldrich (St. Louis, MO, USA). Endotracheal tubes were from Covidien (Mansfield, MA, USA). Microbial reference strains were from American Type Culture Collection (Manassas, VA, USA). Clinical isolates were supplied by Songklanagarind Hospital, Hat Yai, Thailand (Ethical Approval No. REC 59–241–19–6). Culture media for microorganisms were from Becton, Dickinson, and Company (Sparks, MD, USA). Dulbecco's Modified Eagle's Medium (DMEM), fetal bovine serum, and trypan blue stain were purchased from Gibco Laboratories (Grand Island, NY, USA). Twenty-four-well and 96-well cell culture plates were from SPL Life Science (Gyeonggi-do, Republic of Korea). All other chemicals were purchased from Merck KGaA (Darmstadt, Germany) unless otherwise specified.

Coating process

ETT were first rinsed with deionized water and then immersed in silver salt solution. After incubation in darkness

at different diffusion times (1–5 days), the tubes were washed twice with deionized water and placed in a solution of *Eucalyptus camaldulensis* extract for 24 h. The obtained AgNPs-coated ETT were removed from the extract, washed with deionized water, and air-dried.

Characterization of AgNPs-coated ETT

The absorption spectra of AgNPs-coated ETT were recorded by UV–vis spectroscopy, scanning at wavelength range 350–400 nm. The presence of silver elements on the top surface and cross-sections of coated ETT was confirmed by observation of line scans from energy dispersive X-ray spectroscopy (EDX) (Quantax 70, Hitachi, Japan). The size distribution of AgNPs on coated surfaces was determined by analysis of electron micrographs taken at 150,000x magnification by a field emission-scanning electron microscope (FESEM) (Quanta 400, FEI, Netherlands). The photographs were analyzed using ImageJ software. Surface roughness and topology of representative areas of coated surfaces (5 × 5 µm) were examined using atomic force microscopy (AFM) (easyScan 2, Nanosurf, Switzerland) in non-contact mode. The crystalline structure of AgNPs-coated surfaces was identified by X-ray diffraction (XRD) analysis (PANalytical Empyrean, Netherlands).

Anti-planktonic growth and antimicrobial adhesion

The anti-planktonic growth and antimicrobial adhesion properties of the AgNPs-coated ETT were tested against important pathogens causing VAP. The pathogens included *Acinetobacter baumannii* ATCC 19606, carbapenem-resistant *A. baumannii* NPRCoE 1605090, *Escherichia coli* ATCC 25922, extended-spectrum β-lactamase-producing *E. coli* NPRCoE 1610011, *Klebsiella pneumoniae* ATCC 700603, extended-spectrum β-lactamase-producing *K. pneumoniae* NPRCoE 1606111, *Pseudomonas aeruginosa* ATCC 27853, carbapenem-resistant *P. aeruginosa* NPRCoE 1609014, *Enterococcus faecalis* ATCC 29212, *E. faecalis* NPRCoE 1607011, *Staphylococcus aureus* ATCC 25923, methicillin-resistant *S. aureus* 1608011, *Candida albicans* ATCC 90028, and *C. albicans* NPRCoE 1601030. Coated ETT segments were immersed in microbial suspensions and incubated at 37 °C for 24 h. The anti-planktonic properties of the coated ETT were evaluated by colony count of serially diluted microbial suspensions. To determine anti-adhesion effects, ETT samples were removed from the cultures and washed twice with phosphate buffered saline (PBS) to remove non-adherent cells. Attached microorganisms were then extracted from ETT surfaces by placing the samples in 0.9% saline solution, under sonication for 15 min, followed by vortexing for 1 min. The microbial cells in the solution were tenfold serially diluted and plated on agar. Colonies were counted after incubation at 37 °C for 24 h.

Preparation of human tracheal mucus

The antibiofilm activity of the AgNPs-coated ETT was tested in culture medium supplemented with human tracheal mucus to simulate biological conditions. The mucus samples were collected from ETT using a method previously described (Muller et al. 2018; Rubin et al. 1990). Endotracheal tubes were collected from mechanically ventilated patients at the Critical Care Medicine Unit, Songklanagarind Hospital. The protocol was approved by the Human Research Ethics Committee, Faculty of Medicine, Prince of Songkla University (Protocol No. REC 64–341–19–6). After removing the ETT from the patient, approximately 10 cm of the distal portion of the ETT was sectioned and placed in a 50-mL centrifuge tube. Undiluted human tracheal mucus samples were collected by centrifugation. The samples were pooled and weighed before freeze-drying. The freeze-dried samples were sterilized before use by exposure to UV radiation for 1 h and re-hydrated with sterile buffer.

Antibiofilm activity

The effects of the coated ETT on biofilm formation were determined using the crystal violet assay. *Pseudomonas aeruginosa*, *S. aureus*, and *C. albicans* were chosen to represent Gram-negative and Gram-positive bacteria, and fungi, respectively. The AgNPs-coated ETT was challenged with 10^6 CFU/mL of *P. aeruginosa* ATCC 27853 or *S. aureus* ATCC 25923 or *C. albicans* ATCC 90028 in culture medium supplemented with 0.005% v/v of human tracheal mucus. After incubation for 3 days, the coated samples were washed twice with PBS to remove unattached cells. Biofilm mass was determined after staining with 0.1% w/v crystal violet and incubation at room temperature for 1 h. The excess crystal violet solution was washed out, and the remaining crystal violet on the ETT surface was dissolved with dimethyl sulfoxide before optical density was measured at 590 nm. Microbial cell viability in biofilms was quantified using the 3-(4,5-dimethylthiazol-2-yl)-2,5-diphenyltetrazolium bromide (MTT) reduction assay. The presence of microorganisms on material surfaces was observed under a fluorescence microscope after staining the materials with SYTO-9 green-fluorescent nucleic acid dye. Following 3-day incubation in supplemented culture medium, the biofilm architecture on material surfaces was observed under a scanning electron microscope (SEM). To prepare ETT samples for observation, they were rinsed twice with PBS, fixed with 2.5% glutaraldehyde for 6 h, and dehydrated in an alcohol series from 30 to 100% for 15 min each. The samples were then stabilized by critical point drying and coated with gold.

Cytotoxicity test

The cytotoxicity of the AgNPs-coated ETT was determined according to the ISO 10993–5 protocol. First, fibroblast cell line L929 was incubated with an extract obtained by immersing and incubating the coated ETT in DMEM medium supplemented with tracheal mucus at 37 °C for 3 days. L929 cells were cultured in the complete medium supplemented with tracheal mucus and incubated for 24 h at 37 °C in a humidified atmosphere of 5% CO_2. After the cells had reached 80–90% confluence, the growth medium was replaced with the extract and incubation continued for 24 h. Cell viability after the treatment was determined using the trypan blue exclusion assay. Cell metabolic activity was examined using the MTT assay. Optical density was measured at 570 nm. The morphology of L292 cells was observed under an inverted microscope (10x magnification).

Assessment of AgNPs-coated ETT in a porcine VAP model

An animal experiment was conducted in accordance with the Institutional Animal Care and Use Committee at Chulalongkorn University, Thailand (Approval No. 1973017). Five healthy 10-week-old male pigs of mixed breed (*Duroc*×*Landrace*×*Yorkshire*) weighing approximately 25 kg were used. The health of the animals was assessed daily leading up to the experiment. The pigs were sedated by intramuscular injection of 1 mg xylazine/kg combined with 3 mg tiletamine/zolazepam/kg and then anaesthetized via intravenous injection of 4–6 mg propofol/kg. Crystalloid fluid was given intravenously at 5 mL/kg/h to maintain circulation. Anesthesia was maintained in the sternal recumbent position with a heat mat underneath the patient, using 1–3% isoflurane inhalation in 100% oxygen through the ETT. Ventilators were set up at a tidal volume of 10 mL/kg with inspiration–expiration time set at a ratio of 1:3. Vital parameters including oxygen saturation, blood pressure, end-tidal carbon dioxide, and electrocardiography were assessed every 15 min. Metabolic balance, including blood glucose, blood acid–base balance, lactic acid, and electrolytes (sodium and potassium), was monitored every 6 h along with indirect body fluid measurements of pack cell volume and total protein. Kidney parameters (BUN and creatinine) and hepatic parameters (SGPT and ALP) were measured every 24 h.

Pigs were randomly blinded to be intubated either with an AgNPs-coated ETT (experimental group) or uncoated ETT (control group). Immediately after placement of the tube in the trachea, swabs were collected from the trachea, larynx, and buccal mucosa of each animal for enumeration of the normal microbiota baseline. To reflect the key pathogenic mechanisms of VAP in humans, pigs were challenged with *P. aeruginosa* PAO1 introduced into the oropharynx (Bassi et al. 2014). After tracheal intubation, each animal was challenged with *P. aeruginosa* immediately and 4 h thereafter. For each challenge, 5 mL of approximately 10^6 CFU/mL of a log-phase culture of *P. aeruginosa* were slowly instilled into the buccal pouch of the animals.

At the experimental end point (48 h), the animals were euthanized with potassium chloride given intravenously at 1–2 mEq/kg. After that, the ETT was removed from the trachea by tracheostomy to prevent contamination with oral bacteria. Three different segments (5-cm long) of the ETT, including the proximal third, the portion just proximal to the cuff, and the cuffed portion, were cut and placed in 0.85% saline solution. Attached cells were detached from ETT surfaces by sonication. Microbial cell solutions were plated on tryptic soy agar and MacConkey agar to enumerate numbers of total bacteria and *P. aeruginosa*, respectively. Five lung lobes (right upper lobe, right middle lobe, right lower lobe, left upper lobe, and left lower lobe) were removed from each animal for microbiological assessment. Each lung lobe tissue sample was weighed, aseptically prepared, and homogenized in sterile saline solution. Homogenized samples were serially diluted and spread-plated on tryptic soy agar and MacConkey agar.

A randomized controlled trial in veterinary patients

A pilot randomized controlled trial was conducted at the Veterinary Teaching Hospital, Prince of Songkla University, Thailand, to assess the antibacterial efficacy of the AgNPs-coated ETT. The study involved 47 dogs of both sexes, of various ages, breeds, and weights, that were scheduled to undergo a variety of surgical procedures. Informed written consent from owners was obtained prior to animal enrolment, and the study was approved by the Institutional Animal Care and Use Committee, Prince of Songkla University (Protocol No. 2560–05-062).

The physical status of the animals was assessed. The assessments included the results of a physical examination and laboratory data showing complete blood count and serum chemistry profiles. Food and water were withheld for 8 h and 2 h respectively before surgery. All animals received standard premedication before anesthesia was induced. The animals were intubated with an AgNPs-coated ETT or an uncoated ETT in a procedure that was randomly blinded to the anesthesiologist. An inhalation anesthetic of isoflurane (Forane®, Baxter Healthcare Corporation, USA) was used in 100% oxygen through the ETT. Multi-vital sign parameters of body temperature, heart rate, respiratory rate, oxygen saturation, blood pressure, and end tidal carbon dioxide were monitored every 5 min.

At the end of the surgery, ETT were extubated and aseptically collected for quantitative microbiology. Collected ETT were cut into 3 sections, including the proximal, middle, and

distal parts. Each section was placed in a 50-mL centrifuge tube containing 30 mL of 0.85% saline solution. Microorganisms on the surfaces of sections were extracted by sonication for 15 min followed by vortexing for 1 min. Microbial cells in solution were serially diluted and plated on tryptic soy agar to enumerate the total microorganisms.

Results

Characterization

To enable the synthesized AgNPs to adhere to both inner and outer ETT surfaces and penetrate the tube material, *E. camaldulensis* extract was added as a reducing and stabilizing agent (Fig. 1A). The diffusion time used to coat the ETT with AgNPs changed the appearance of the ETT (Fig. 1B). The presence of AgNPs on the coated ETT was investigated by UV–vis spectroscopy. All spectra presented an absorption peak at ~490 nm (Fig. S1). The inset in Fig. S1 displays the evolution of absorption peak intensity with diffusion time of silver ions.

EDX spectroscopy showed that the highest surface deposition of AgNPs and deepest penetration (about 20 μm) were presented by the ETT immersed in silver solution for 5 days (Fig. 2A). The results were consistent with the optical images of the cross-sections of various tube (Fig. 2B).

Since the ETT immersed in silver solution for 5 days had the most AgNPs embedded on the surface and inside the tube medium, it was selected for further investigation. The size and size distribution of AgNPs were revealed by SEM. Most AgNPs appeared in aggregations composed of smaller primary AgNPs (Fig. 3A). The size distribution of primary particle diameters was from about 10 to 60 nm (Fig. 3B). The mean size of AgNPs on the coated surface was 28 ± 9 nm. The surface topography of the AgNPs-coated ETT was examined using AFM. The average root-mean-square roughness of the surface was 31 ± 8 nm with a peak-to-valley distance of about 141 ± 55 nm (Fig. 3C). The XRD pattern of the AgNPs-coated ETT was generally similar to the pattern of the uncoated ETT (Fig. 3D).

Anti-planktonic growth and antimicrobial adhesion

The antimicrobial activity of the AgNPs-coated ETT against VAP pathogens was evaluated by assessing the amount of planktonic growth and adhered microorganisms on the material surfaces. Following 24 h incubation, compared with the uncoated ETT, the coating significantly reduced free-floating organisms by 3.6–5.2 log CFU/mL for Gram-negative bacteria, 2.8–3.6 log CFU/mL for Gram-positive bacteria, and approximately 3.0 log CFU/mL for fungi ($p < 0.05$) (Fig. 4A and B). Moreover, significantly lower cell adhesion to the AgNPs-coated surface was observed in all the tested pathogens ($p < 0.05$). The reductions in numbers of adhered Gram-negative, Gram-positive bacteria, and fungi ranged from 2.0 to 4.3 log CFU/mL (Fig. 4C and D).

Kinetic adhesion

To better understand the antimicrobial effects of the AgNPs-coated ETT, the kinetic adhesion of pathogens to the material surface was investigated. The coating exhibited strong activity against *P. aeruginosa* adhesion (Fig.5A). No increase in adhesion was detected on the coated surface during 12-h exposure, while an increase of more than 4 log CFU/mL was found on the uncoated ETT surface. A gradual increase in *S. aureus* adhesion to the uncoated ETT was observed (Fig. 5B) but numbers of *S. aureus* on the coated ETT were more than 2 log CFU/mL lower within 4 h and remained almost unchanged over the following 20 h. The attachment of *C. albicans* to the AgNPs-coated surface

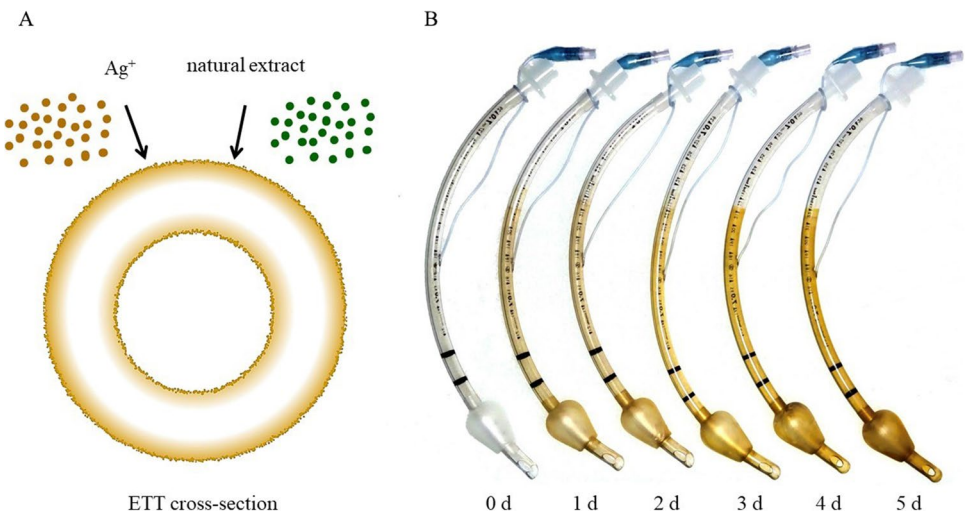

Fig. 1 The diagram illustrates the endotracheal tube coating process based on the diffusion of silver ion precursors into the tube medium at both inner and outer surfaces, followed by immersion in a natural reducing agent (**A**). Photographs show the increasing color intensity of the AgNPs coating with increments of silver diffusion times (**B**)

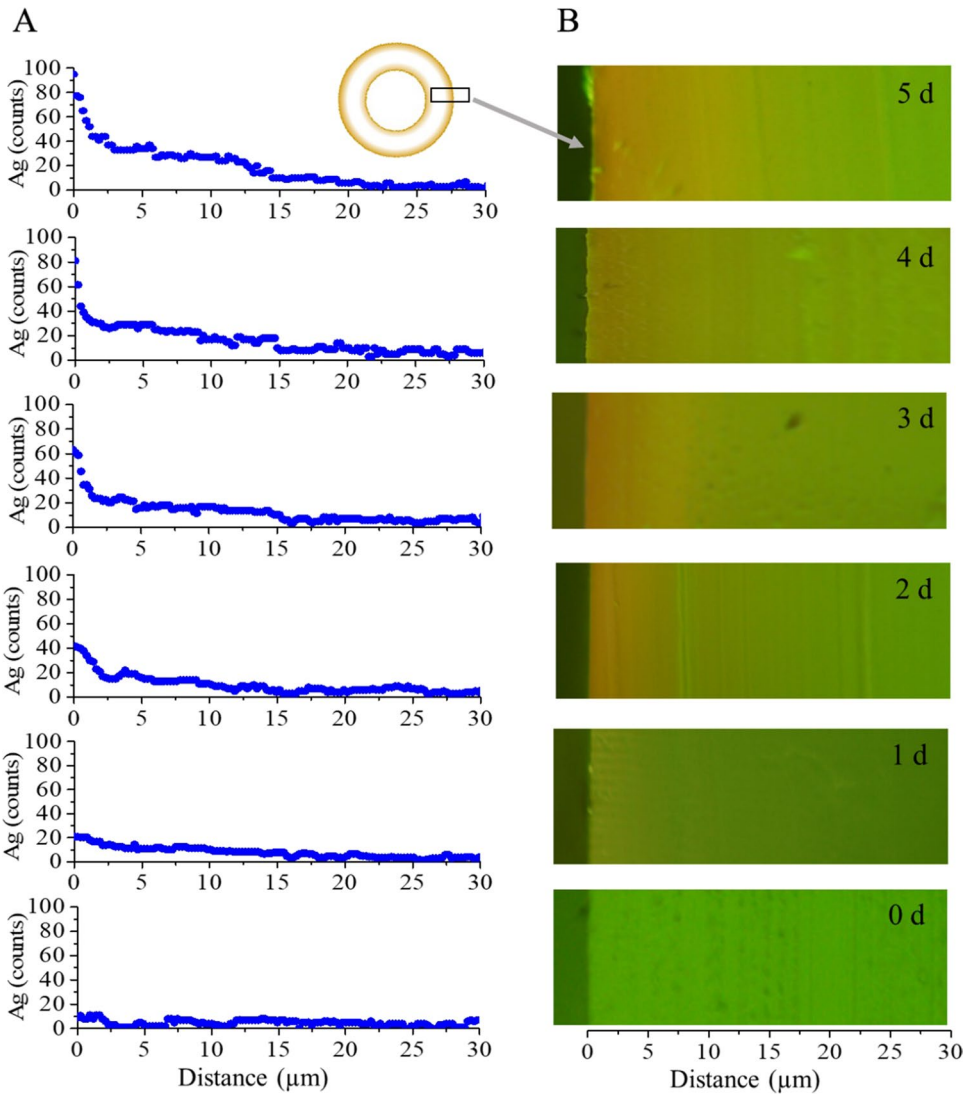

Fig. 2 Energy dispersive X-ray spectroscopy of cross-sections of endotracheal tube demonstrates the intensity of deposited Ag measured from the surface down to a depth of 30 μm (**A**). All data were collected from endotracheal tubes fabricated with diffusion times of 0–5 days. Optical images are of the corresponding tube cross-sections (**B**). Impregnated silver is indicated by yellowish-brown areas while the green area indicates an absence of silver content

compared to the uncoated tube was inhibited by approximately 2 log CFU/mL from 6 h of incubation on throughout the test period (Fig.5C).

Antibiofilm formation

Biofilm biomass after treatment was quantified using the crystal violet assay. After incubation for 3 days, the biofilm mass of each microorganism tested on the AgNPs-coated ETT was significantly smaller than the mass of each robust biofilm observed on the uncoated ETT ($p < 0.05$). The biofilm formation of *P. aeruginosa*, *S. aureus*, and *C. albicans* was inhibited by 78, 76, and 66%, respectively (Fig. 6A). The viability of cells in biofilms was then determined via the MTT assay. The AgNPs-coated ETT reduced the bioactivity of *P. aeruginosa*, *S. aureus*, and *C. albicans* by 93, 77, and 95%, respectively, compared with the uncoated ETT (Fig. 6B).

To confirm the presence of microorganisms on the material surface, biofilms were stained with SYTO-9, a green-fluorescent nucleic acid dye. Under the fluorescence microscope, the cell aggregation of *P. aeruginosa* in the presence of extracellular DNA was observed as a faint haze on the uncoated material. In contrast, no bacterial cells were detected on the AgNPs-coated ETT (Fig. 6C). Large numbers of aggregated *S. aureus* were observed on the uncoated ETT, but only a slight aggregation was established on the coated ETT. *C. albicans* was present on the uncoated surface while the fungal cells were unable to colonize the coated ETT.

Biofilm architectures were revealed by SEM. The results confirmed the antibiofilm properties of the AgNPs-coated ETT. The very small numbers of the tested microorganisms with no glycocalyx were observed on the coated surface. In contrast, the uncoated ETT allowed bacteria and fungi to attach to the surface and establish biofilms. Large numbers of microorganisms

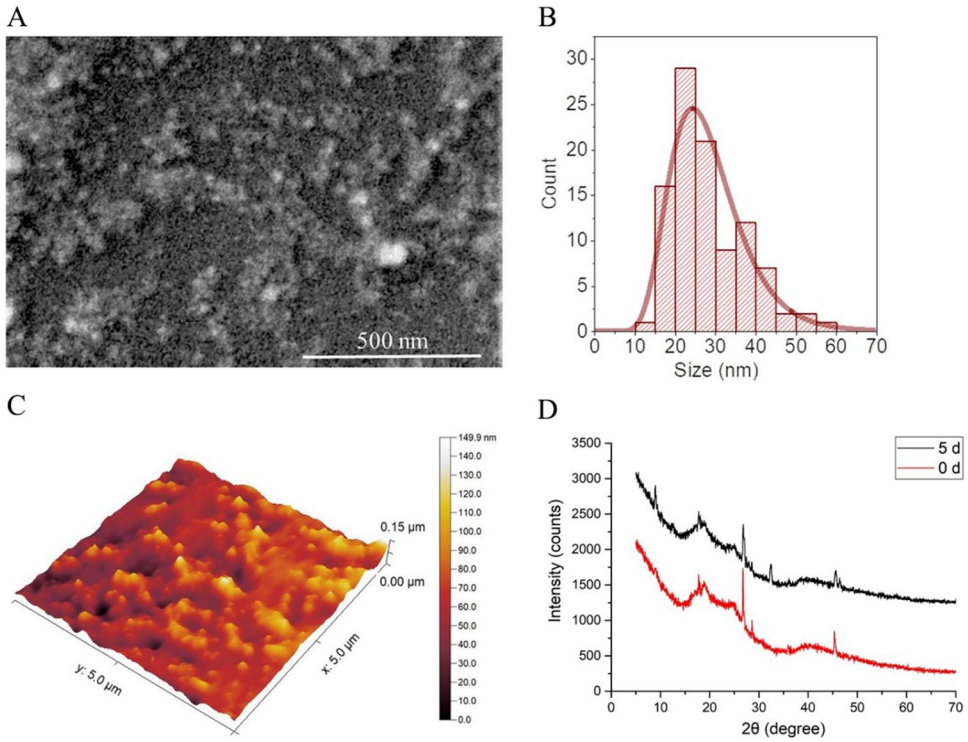

Fig. 3 The surface of an endotracheal tube coated with AgNPs for 5 days was morphologically characterized. The SEM image shows the AgNP distribution on the coated surface (**A**). The histogram of the size distribution of the individual particles shows that the average diameter of AgNPs was 28 ± 9 nm (**B**). The coated surface was scanned by atomic force microscopy (**C**). XRD patterns are of a coated endotracheal tube and an uncoated endotracheal tube (**D**)

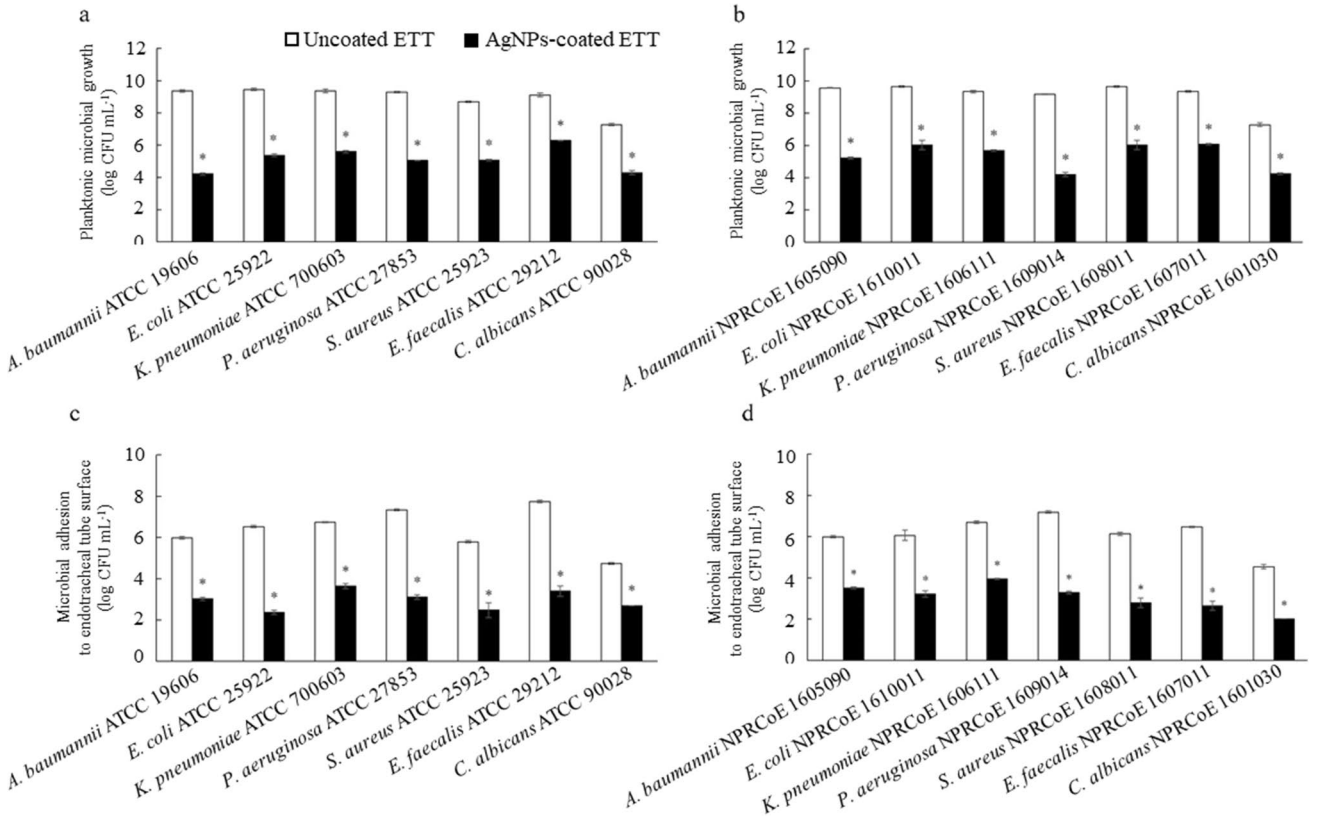

Fig. 4 The antimicrobial activity of the AgNPs-coated endotracheal tube was determined against pathogenic microorganisms after 24 h incubation. Charts show planktonic growth of reference strains (**A**) and clinical isolates (**B**); and microbial adhesion of reference strains (**C**) and clinical isolates (**D**) to the endotracheal tube surface. The limit of detection was 100 CFU/mL. The values are means ± SD from three independent experiments performed in triplicate, $p < 0.05$

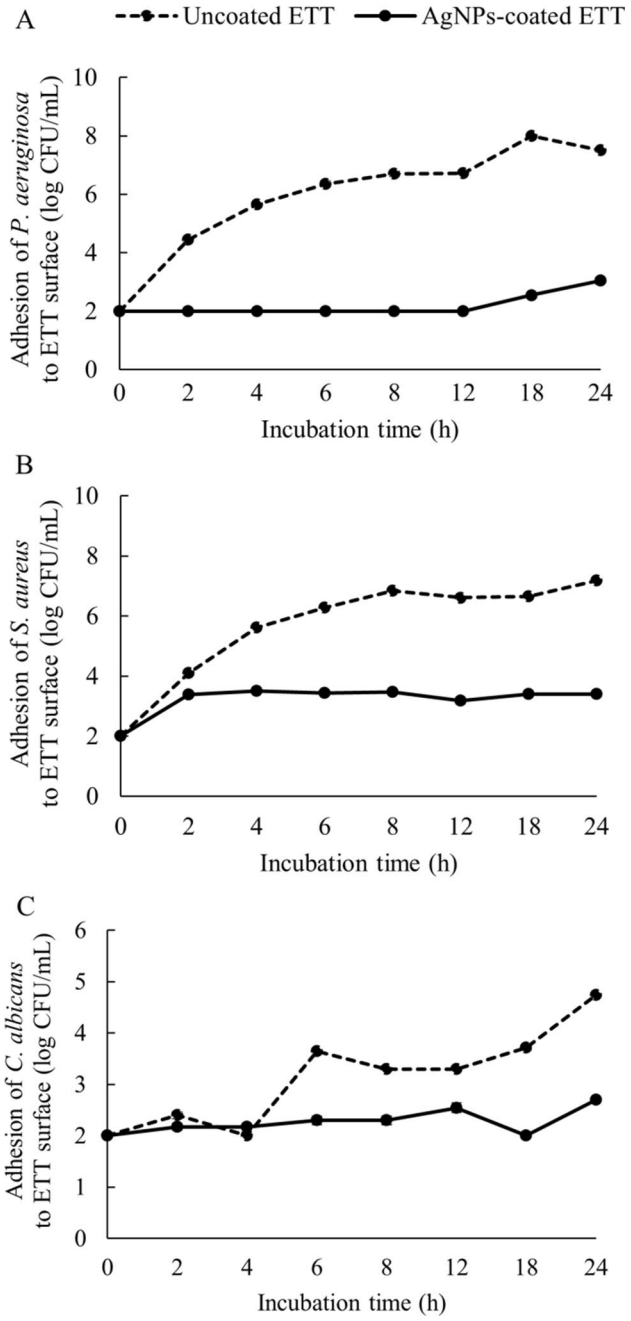

Fig. 5 Charts show kinetic adhesion of *P. aeruginosa* (**A**), *S. aureus* (**B**), and *C. albicans* (**C**) to the endotracheal tube surface. Cultures of 10^6 CFU/mL were incubated with endotracheal tube sections for 24 h. The limit of detection was 100 CFU/mL. The values are means ± SD from three independent experiments performed in triplicate

and well-developed biofilm matrices were present on the uncoated ETT after co-incubation for 3 days (Fig. 6D).

Cytotoxicity

Any novel antimicrobial biomaterial presents a risk of cytotoxicity. To ensure the safety of the AgNPs-coated ETT, biocompatibility was tested using an indirect method. Fibroblast cells are commonly found in the human respiratory system and the L929 fibroblast cell line has been widely used in the ISO 10993 protocol to test for cytotoxicity of novel biomaterials. We obtained an AgNPs extract by immersing the coated ETT in DMEM medium for 3 days. The extract was inoculated into wells of a 96-well plate containing a confluent monolayer of the L929 cell line and the plate was incubated for 24 h. Cell viability was determined using the trypan blue exclusion assay. The non-cytotoxicity of the extract on L929 cells was demonstrated with a cell viability of more than 80% (Fig. 7A). Similar results were obtained from an MTT metabolic activity assay (Fig. 7B). Under the light microscope, no significant change in cellular morphology was observed. Cells exhibited the typical spindle-like shape and oval flat nucleus of healthy L929 cells (Fig. 7C).

Antibacterial activity of AgNPs-coated ETT in porcine model

To demonstrate the efficacy of the AgNPs-coated ETT in vivo, a porcine model of VAP was set up, using *P. aeruginosa* to challenge the oropharynx. Prior to intubation, bacterial cultures taken from the buccal cavity and larynx showed that the pigs were colonized by normal microbiota, but free of *P. aeruginosa* (Table S1).

On day 2 post-intubation, *P. aeruginosa* was not recovered from proximal sections of the coated ETT from all animals. However, the inoculated organism was detected in the middle and distal parts of the coated ETT in one animal. In the control group, *P. aeruginosa* had colonized all parts of the uncoated ETT (10^2 to 10^6 CFU/cm^2) (Table 1).

The *P. aeruginosa* burden in lung tissue samples taken at necropsy is shown in Table 2. No bacterial colonization of lung tissue was detected in animals intubated with the coated ETT. In contrast, lung tissues of animals in the control group were colonized. The average *P. aeruginosa* colonization in lung tissues of the control group was 6.6×10^3 CFU/g. No differences in *P. aeruginosa* colonization were observed in different parts of lung tissues.

A randomized controlled trial

To establish the efficacy and safety of the AgNPs-coated ETT, a randomized clinical trial was conducted at the Veterinary Teaching Hospital, Prince of Songkla University. Forty-seven intubated dogs were included in the study. The duration of intubation was not significantly different between the test group that was intubated with AgNPs-coated ETT and the control group intubated with uncoated

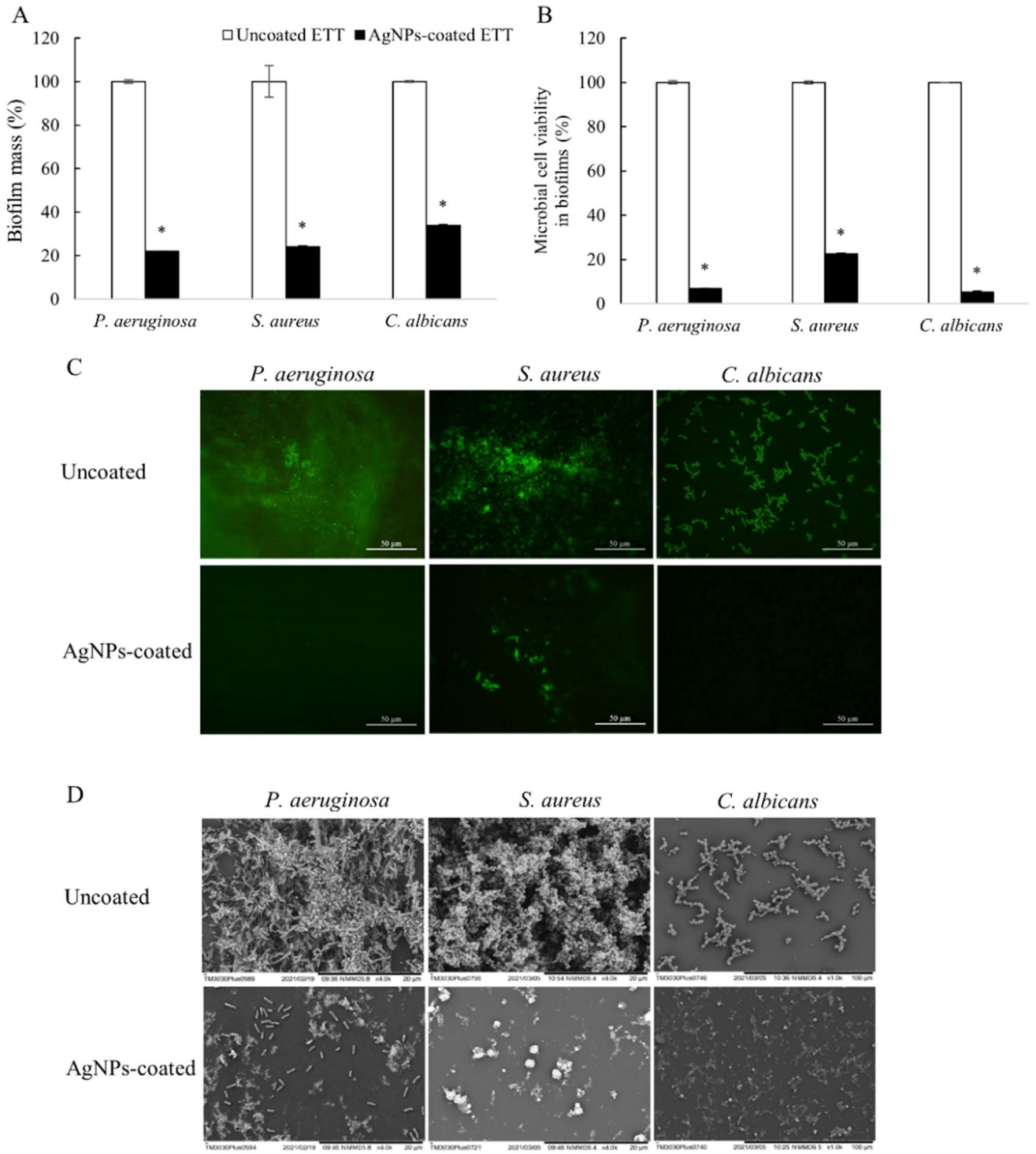

Fig. 6 The effect of the AgNPs-coated endotracheal tube on biofilm formation was investigated following incubation for 72 h with *P. aeruginosa*, *S. aureus*, and *C. albicans*. Biofilm mass was quantified using the crystal violet assay (**A**). Microbial cell viability in biofilms was measured via the MTT assay (**B**). The presence of microbial cells on endotracheal tube surfaces was confirmed by fluorescent images (**C**). Biofilm architecture was observed under the scanning electron microscope (**D**). The values are means ± SD from three independent experiments performed in triplicate, $p < 0.05$. The representative photographs were taken from three independent examinations

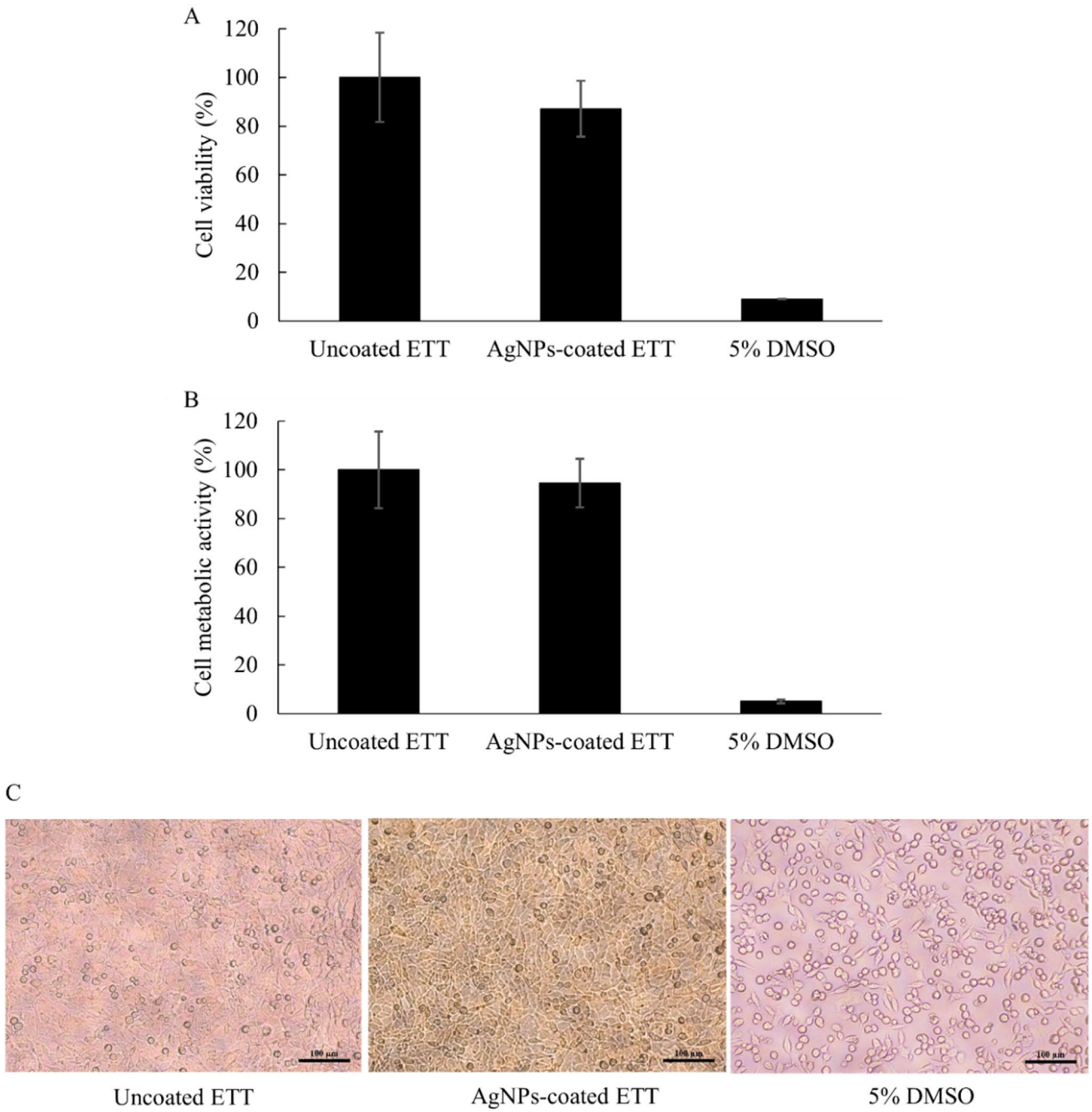

Fig. 7 The cytotoxicity of the AgNPs-coated endotracheal tube was assessed on L929 fibroblast cells following treatment for 24 h with an extract obtained by soaking the coated endotracheal tube in medium for 3 days. Cell viability was studied using the trypan blue exclusion assay (**A**). Cell metabolic activity was determined via the MTT assay (**B**). Fibroblast cell morphology was observed under the optical microscope (10x magnification) (**C**). Cells treated with 5% DMSO were used as a positive control. The values indicate means ± SD from three independent experiments performed in triplicate. The representative photographs were taken from three independent examinations

ETT. There was no report of adverse effects or evidence of toxicity. A significant difference was observed between the microbial burdens on different parts of AgNPs-coated ETT and uncoated ETT ($p < 0.05$). Within the test and control groups, higher numbers of microorganisms were present on the distal end of the ETT (Fig. 8A). The total number of microorganisms was significantly lower on the surfaces of AgNPs-coated ETT than uncoated ETT (1.5×10^5 vs 1.0×10^4 CFU/mL, $p < 0.05$) (Fig. 8B). The results demonstrated more than a 90% reduction of

Table 1 Recovered *Pseudomonas aeruginosa* from different parts of endotracheal tube

	Porcine No	Recovered *Pseudomonas aeruginosa* (CFU/cm^2)		
		Proximal	Middle	Distal
AgNPs-coated ETT	1	-[a]	8.2×10^4	2.0×10^5
	2	-	-	-
	3	-	-	-
Uncoated ETT	4	4.9×10^3	3.7×10^2	1.6×10^5
	5	3.3×10^4	5.3×10^4	3.7×10^6

[a]No *Pseudomonas aeruginosa* colonization was detected

bacterial adhesion on the surfaces of the AgNPs-coated ETT.

Discussion

Several strategies to reduce the incidence of VAP have been studied. One of the most effective interventions is the use of biofilm-resistant ETT with modified surfaces to prevent the adhesion of microbial cells, a vital step in biofilm formation during VAP pathogenesis. Generally, antimicrobial coatings or surfaces can be classified as active or passive. Active coatings, or biocidal surfaces, are surfaces that kill microorganisms either with immobilized antimicrobial agents or by the release of an antimicrobial compound from the material surface to the environment. Passive coatings are surfaces that discourage microbial cell adhesion and prevent the attachment of cell debris and proteins. The presence of dead cells on antimicrobial surfaces can hinder the antimicrobial activity of the surfaces by facilitating microbial attachment and biofilm formation (Su et al. 2021). A robust biofilm was found to have more dead cells than a weak biofilm since dead bacterial cells represent a major source of extracellular DNA, one of the main components of biofilm (Desai et al. 2019).

In this study, the antimicrobial and antifouling functionalization of an ETT was successfully achieved by immersing the ETT in silver solution for 5 days. The numbers of trials for depositing the biogenic AgNPs on ETT surfaces had been studied in order to select the most suitable condition giving the best physical properties for further biological activity investigation. The formation and deposition of AgNPs on the tube surfaces changed the appearance of the transparent ETT, which became yellowish-brown when coated. Longer immersion times increased the impregnation with AgNPs and the color became darker with time. The presence of AgNPs on the coated surfaces was confirmed by UV–vis spectroscopy. The absorption spectrum presented at ~491 nm corresponded to the surface plasmon resonance of AgNPs (Rehan et al. 2020). The data points in Fig. S1 fitted well with the exponential function, indicating the slowing rate of deposition as the silver loading was reaching saturation.

Broadened absorption spectra with a slight red shift may result from the presence of AgNPs aggregations (Ferrer et al. 2012; Wang et al. 2019). The increase in absorbance confirmed that more AgNPs were deposited on the tube material with immersion time (Rivero et al. 2011). EDX line scanning of cross-sections of ETT was used to determine the depth to which AgNPs diffused into the tube material. The AgNPs were highly concentrated near the surface of the coated ETT and the concentration decreased gradually into the tube material. When diffusion time was prolonged, larger amounts of AgNPs were observed on the surface of the ETT and the penetration of AgNPs into the material of the ETT increased.

The sizes of AgNPs on coated substrates can vary depending on the coating method and reducing agent used in the process. An in situ approach to developing polyurethane/silver-nanocomposites produced larger particles than an ex situ method, as the high temperature of the in situ process caused particle agglomeration (Triebel et al. 2011). A large particle size, ranging from 50 to 800 nm, was observed on a catheter coated with AgNPs, using polydopamine as a reducing agent (Zhang et al. 2019). The particle size of synthesized AgNPs is an

Table 2 Recovered *Pseudomonas aeruginosa* from pulmonary lobes

	Porcine No	Recovered *Pseudomonas aeruginosa* (CFU/g^1)				
		Right upper lobe	Right middle lobe	Right lower lobe	Left upper lobe	Left lower lobe
AgNPs-coated ETT	1	-[a]	-	-	-	-
	2	-	-	-	-	-
	3	-	-	-	-	-
Uncoated ETT	4	5.2×10^3	4.7×10^3	3.1×10^3	7.2×10^3	4.0×10^3
	5	7.5×10^3	3.1×10^3	3.8×10^3	7.9×10^3	2.0×10^4

[a]No *Pseudomonas aeruginosa* colonization was detected

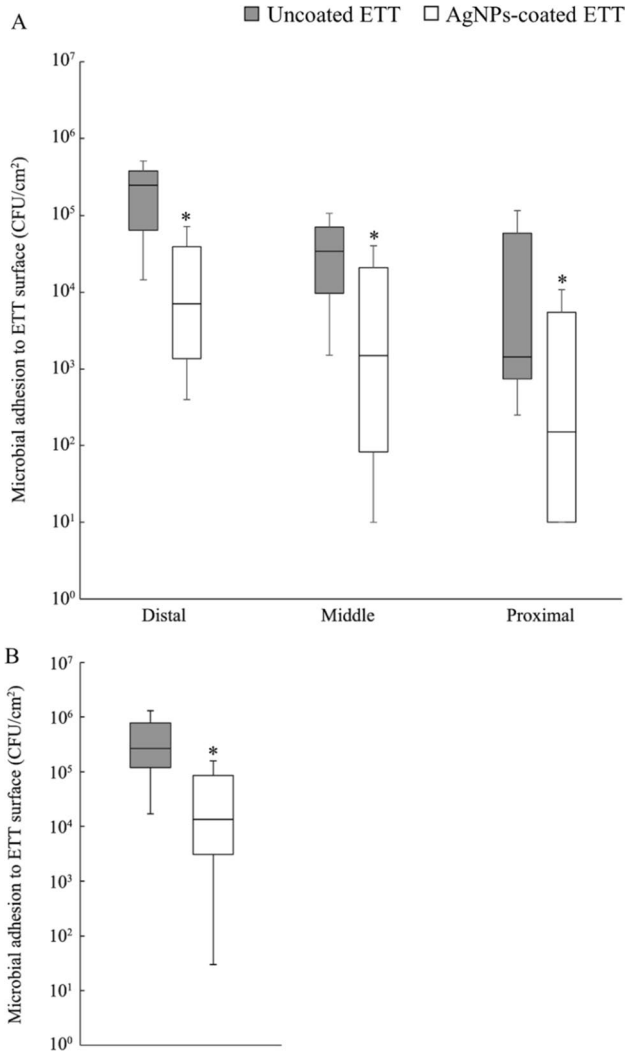

Fig. 8 Microorganisms were isolated from uncoated and AgNPs-coated endotracheal tubes collected from 47 mechanically ventilated dogs that underwent a variety of surgical interventions. Microorganisms isolated from different parts of endotracheal tubes (**A**) and total numbers of microorganisms from endotracheal tube surfaces (**B**) were counted on tryptic soy agar. Boxes are 25th to 75th percentiles. Solid lines within the boxes represent the 50th percentile. Capped bars represent 10th and 90th percentiles, $p < 0.05$

important consideration since the biological effects of nanoparticles are directly related to their size. Small AgNPs have demonstrated strong antimicrobial activities as they present a large surface area to bind with bacteria. The results of the present study agreed well with the finding of our previous study that successfully synthesized small AgNPs of approximately 8.65 nm, using *E. camaldulensis* leaf extract as a reducing and capping agent (Wunnoo et al. 2021). The process to synthesize AgNPs used in this study differed from the previous study in that there was no centrifugation step to remove excess silver and plant extract solution. Instead, the coated ETT were air-dried. Any remaining excess solutions could produce larger particles and aggregations of AgNPs on the coated surface, which may have resulted in the slight red shift of the absorption peak in the UV–vis spectra.

The nanostructured surface roughness of the coated ETT could be attributed to the continuous impregnation of nanoparticles on the material surface. Increased surface roughness was also observed by Zhang et al. (2021) after depositing AgNPs on a smooth substrate surface. Surface topography is considered one of the main factors involved in bacterial adhesion and biofilm formation. Materials with high surface roughness are generally less favorable for microbial cell attachment. Singh et al. (2011) found that a biomaterial surface with a root-mean-square roughness of 32.2 nm showed little bacterial aggregation, while a thick biofilm formed on a surface with a root-mean-square roughness of about 16.2 nm. However, some studies have reported that high surface roughness resulted in increased microbial adhesion (Yu et al. 2016). Surface microstructures could provide a large total surface area for bacterial cell attachment and promote microbial accumulation by protecting the cells from shear forces (Scheuerman et al. 1998). Conversely, a surface nanostructure that presents a large peak-to-valley distance and high peak density could present contact areas smaller than bacterial cells. As a result, surface area could be small and bacterial adhesion low (Wu et al. 2018).

The AgNPs-coated ETT was then analyzed by XRD to confirm the presence of silver on the material surface. The similarity between the patterns of the uncoated and AgNPs-coated ETT could be due to the amorphous nature of the PVC-based ETT. However, by comparison with the pattern of the uncoated ETT, the peak intensity of the pattern of the coated ETT was lower; probably due to the coating of AgNPs on the ETT surface. LewisOscar et al. (2021) attributed peak patterns with 2θ of ~32° and ~46° to the presence of silver on the coated materials analyzed and XRD analysis indicated to Gurunathan et al. (2014) that AgNPs on the coated surface were crystalline with a face-centered cubic structure.

The pronounced antimicrobial activity of the AgNPs-coated ETT against planktonic microorganisms was achieved by releasing AgNPs from the coated surface to directly kill pathogens in the surrounding environment. AgNPs can kill microorganisms via several mechanisms that have been described in many studies. Generally, smaller AgNPs are more effective because they will bind to a larger surface area of the microbial cell. They can then disturb membrane permeability, penetrate cells (Paosen et al. 2019), and interact with DNA, causing cell death (Wintachai et al. 2019).

Interactions between microbial cells and substrates depend on surface physicochemical properties such as charge, polarity, and topography. When microorganisms that survive antimicrobial compounds are close to material

surfaces, the first important force that enables microbial attachment to the surfaces is Van Der Waals interaction (Rutter 1980). Bacterial cells have an overall negative charge. In Gram-negative bacteria, the charge is due to the presence of lipopolysaccharides bacteria, and in Gram-positive bacteria, it is due to teichoic acid. The cell surfaces of *C. albicans* also possess a negative charge from sialic acid, which determines its surface interactions (Soares et al. 2000). The AgNPs-coated ETT exhibited pronounced anti-adhesion activity toward both bacteria and the fungus. This activity could be attributed to the negatively charged embedded AgNPs (Wunnoo et al. 2021), which produced an overall negative charge on the ETT surface. The negative charges of the microbial cells and ETT surface repelled each other; therefore, the coating can potentially prevent the attachment of microorganisms by electrostatic repulsion. The AgNPs on the ETT surface demonstrated anti-planktonic activities by releasing silver ions and AgNPs to kill microbial cells in the surrounding solution, and could prevent microbial cell adhesion by electrostatic repulsion. Therefore, the AgNPs exhibited antimicrobial properties by acting as an active coating, and antifouling properties by acting as a passive coating.

Biofilm on an ETT surface represents a significant source of the microbial colonization responsible for VAP. Extracellular biofilm matrix can limit the antimicrobial mechanisms not just of antimicrobial compounds but also of host immune responses and the treatment of infections subsequently becomes more difficult. Therefore, the use of materials with antibiofilm properties is an ideal approach to reducing the incidence of device-associated infections. The antibiofilm activity of the proposed AgNPs-coated ETT against important VAP-associated pathogens was evaluated over 72 h in the presence of human tracheal mucus. The AgNPs-coated ETT provided strong protection against microbial adhesion by inhibiting microbial cell attachment to the ETT surface. The differences in time required for preventing microbial adherence to the coated surface of Gram-negative, Gram-positive bacteria, and fungi are probably due to the differences in their cell structure. Thick peptidoglycan layers of Gram-positive bacterial cell wall may act as a barrier to prevent penetration of the AgNPs through the cell, compared with Gram-negative bacteria which have thinner peptidoglycan. *Candida albicans*, a eucaryotic organism has more complex cell structure than bacteria. The complexity of fungal cell structure may play an important role in their sensitivity to the coated tubes (Wunnoo et al. 2021).

In VAP, the colonization of ETT surfaces by pathogens is likely associated with exposure to environmental mucus. In order to simulate this condition, antibiofilm activities were tested in culture medium supplemented with human tracheal mucus isolated from ETT used by hospital patients supported with mechanical ventilation. The presence of mucin, a major component of mucus, can modulate microbial pathogenesis. *Pseudomonas aeruginosa* utilizes monosaccharides in mucin as binding sites and a carbon source (Hoffman et al. 2020). The twitching motility and biofilm formation of *P. aeruginosa* was reported to be promoted in culture medium containing sputum (Diaz Iglesias and Van Bambeke 2020) and the antimicrobial effects of antibiotics may be hindered by the presence of mucus. Polycationic antimicrobial agents such as polymyxin and tobramycin were reported to lose their efficacy after binding with polyanionic glycoproteins of mucin present in sputum (Muller et al. 2018; Samad et al. 2019).

The strong antibiofilm activity of the AgNPs-coated ETT was not affected by the presence of mucus. During this investigation, the antibiofilm property of the AgNPs-coated ETT was attributed to two types of activity. Pathogens were killed by contact with silver ions released from AgNPs or by AgNPs on the ETT, and bacterial adhesion was prevented by electrostatic repulsion. The study of antibiofilm activity in human tracheal mucus showed that the negatively charged phyto-mediated synthesized AgNPs could not bind to the glycoproteins present in mucus. Therefore, the maximum potential of the AgNPs-coated ETT to prevent biofilm formation and kill microorganisms was unaffected and the high level of antipathogenic activity maintained.

The synthesis of the AgNPs was designed to improve antimicrobial effects and stability and reduce toxicity to human cells. Very recently, we demonstrated that AgNPs synthesized using *E. camaldulensis* as a reducing and capping agent produced small nanoparticles of approximately 8.65 nm. The synthesized AgNPs showed good antimicrobial activities with no cytotoxic effects on HeLa cells (Wunnoo et al. 2021). Green-synthesized AgNPs have been studied for applications in food packaging materials (Nwabor et al. 2020), and have been used as a coating agent on gloves to prevent microbial transmission (Paosen et al. 2021), and on sutures to prevent surgical site infections (Syukri et al. 2021).

According to the ISO 10993 protocol, a remaining viability of treated cells higher than 70% indicates a non-cytotoxic agent. Taken together, the results suggest that the proposed AgNPs-coated ETT is a biocompatible material with no cytotoxic effects toward mammalian cells. The demonstrated potential of the AgNPs-coated ETT to inhibit microbial colonization and biofilm formation was further investigated in an animal model and clinical setting.

The antimicrobial efficacy of different antimicrobial-coated ETT has been reported by a few studies that used animal models but rodents are widely used for these types of in vivo experiments. An ETT coated with sphingosine, an antimicrobial lipid, inhibited *P. aeruginosa* and *S. aureus* colonization by about 10^4 CFU/mL in mouse lung tissue after 45 min intubation (Seitz et al. 2019). A study using a

rabbit model demonstrated that after 16 h, a silver-coated ETT reduced the *P. aeruginosa* burden on the ETT surface by approximately 3 log CFU/mL compared with an uncoated ETT (Rello et al. 2010). However, using small mammal models may not reproduce the pathophysiology of pneumonia in humans accurately enough since the experiments are often performed without mechanical ventilatory support or an adequate intubation time (Mizgerd and Skerrett 2008). The efficacy of new biomaterials is increasingly investigated using larger animals such as sheep, dogs, primates, and pigs as they are closer to humans anatomically, physiologically, and genetically. Despite the limitations posed by the cost and availability of facilities, using a large animal model could represent an excellent approach to studying the performances of a novel antimicrobial-coated medical device to prevent an infectious disease. *Pseudomonas aeruginosa* was used as a representative strain to induce VAP in a porcine model because it is an opportunistic pathogen associated with several serious infections in humans. It can attach and rapidly form robust biofilms on various surfaces, including indwelling medical devices. In addition, VAP caused by *P. aeruginosa* has been associated with high mortality rates (Brewer et al. 1996). In the present study, although the presence of *P. aeruginosa* was observed in the middle and distal parts of the coated ETT, the microorganism was not detected in lung tissue. It may be that the AgNPs prevented bacterial cells from entering the lower respiratory tract. It also has to be said that individual host immunity plays an important role in defense mechanisms to eradicate microorganisms, and that immunocompromised patients are more likely to develop VAP (Lisboa et al. 2008; Rutter et al. 2011).

VAP is also a serious problem in animals that can result in high morbidity and mortality. It is a common complication when animals receive mechanical ventilation (Bruchim et al. 2014; Fox et al. 2021; Rutter et al. 2011). The etiology of VAP in animals has implicated similar groups of microorganisms to those that cause VAP in humans, *P. aeruginosa*, *E. coli*, *Streptococcus* sp., *Enterococcus* sp., *K. pneumoniae*, and *Acinetobacter* sp., and the treatment of infections is complicated by the multidrug resistance of most of the implicated pathogens (Fox et al. 2021; Rutter et al. 2011).

The highest bacterial burden on the surfaces of both uncoated and coated ETT was found at the distal end of the tube in our study of veterinary patients. This finding was consistent with the findings of several previous studies that reported larger amounts of biofilm around the cuff (Adair et al. 1999; Zur et al. 2004). After intubation, microorganisms accumulate rapidly at the distal end of the ETT, especially around the cuff. The microorganisms can easily become detach and migrate to lung tissue, causing VAP (Oikkonen and Aromaa 1997). The present study has proposed an AgNPs-coated ETT that inhibited colonization of the ETT by pathogenic microorganisms and could reduce the risk of VAP. This is the first report of a novel antimicrobial-coated ETT used in a preventive strategy to reduce the risk of VAP in veterinary patients. Further studies in clinical settings are needed to investigate the safety of the developed AgNPs-coated ETT and its efficacy in preventing VAP in human patients.

In summary, the novel antimicrobial-coated ETT exhibited broad-spectrum antimicrobial activity against Gram-positive and Gram-negative bacteria, and fungi, including multidrug-resistant clinical isolates. In vitro studies mimicking the micro-environment of human trachea demonstrated that planktonic growth, microbial adhesion, and biofilm formation were reduced by the presence of the AgNPs-coated ETT. Supporting data from animal studies encourage further clinical trials to determine the potential of the modified device to prevent the occurrence of VAP in humans.

Supplementary Information The online version contains supplementary material available at https://doi.org/10.1007/s00253-022-12327-w.

Author contribution SL: conceptualization, validation, methodology development, investigation, formal analysis, data processing, project administration, writing original draft preparation, review and editing, visualization. JS: methodology, investigation. CW: methodology, investigation. SD: methodology, investigation. RS: investigation. SW: investigation. SP: investigation. SPV: conceptualization, project administration, resources, review and editing, funding acquisition. KD: conceptualization, project administration, resources, review and editing. CD: conceptualization, project administration, methodology, investigation, resources, review and editing, visualization. All authors read and approved the manuscript.

Funding This work was supported by the National Research Council of Thailand (grant No. N41A640071) and Research and Researcher for Industry-RRI PhD Program (grant No. PHD60I0016).

Data availability The authors declare that the data supporting the findings of this study are available within the article and its supplementary information files.

All applicable national and institutional guidelines for the care and use of animals were followed, and all procedures performed in studies involving human participants were in accordance with the ethical standards of the national research committee, and with the 1964 Helsinki declaration and its later amendments or comparable ethical standards.

Declarations

Competing interests The authors declare no competing interests.

References

Adair CG, Gorman SP, Feron BM, Byers LM, Jones DS, Goldsmith CE, Moore JE, Kerr JR, Curran MD, Hogg G, Webb CH, McCarthy GJ, Milligan KR (1999) Implications of endotracheal tube biofilm for ventilator-associated pneumonia. Intensive Care Med 25:1072–1076. https://doi.org/10.1007/s001340051014

Bassi GL, Rigol M, Marti JD, Saucedo L, Ranzani OT, Roca I, Cabanas M, Munoz L, Giunta V, Luque N, Rinaudo M, Esperatti M, Fernandez-Barat L, Ferrer M, Vila J, Ramirez J, Torres A (2014) A novel porcine model of ventilator-associated pneumonia caused by oropharyngeal challenge with *Pseudomonas aeruginosa*. Anesthesiology 120:1205–1215. https://doi.org/10.1097/ALN.0000000000000222

Bonell A, Azarrafiy R, Huong VTL, Viet TL, Phu VD, Dat VQ, Wertheim H, van Doorn HR, Lewycka S, Nadjm B (2018) A systematic review and meta-analysis of ventilator-associated pneumonia in adults in Asia: an analysis of national income level on incidence and etiology. Clin Infect Dis 68:511–518. https://doi.org/10.1093/cid/ciy543

Brewer SC, Wunderink RG, Jones CB, Leeper KV (1996) Ventilator-associated pneumonia due to *Pseudomonas aeruginosa*. Chest 109:1019–1029. https://doi.org/10.1378/chest.109.4.1019

Bruchim Y, Aroch I, Sisso A, Kushnir Y, Epstein A, Kelmer E, Segev G (2014) A retrospective study of positive pressure ventilation in 58 dogs: indications, prognostic factors and outcome. J Small Anim Pract 55:314–319. https://doi.org/10.1111/jsap.12211

Chang R, Elhusseiny KM, Yeh YC, Sun WZ (2021) COVID-19 ICU and mechanical ventilation patient characteristics and outcomes-a systematic review and meta-analysis. PLoS ONE 16:e0246318. https://doi.org/10.1371/journal.pone.0246318

Daengngam C, Lethongkam S, Srisamran P, Paosen S, Wintachai P, Anantravanit B, Vattanavanit V, Voravuthikunchai S (2019) Green fabrication of anti-bacterial biofilm layer on endotracheal tubing using silver nanoparticles embedded in polyelectrolyte multilayered film. Mater Sci Eng C 101:53–63. https://doi.org/10.1016/j.msec.2019.03.061

Desai S, Sanghrajka K, Gajjar D (2019) High adhesion and increased cell death contribute to strong biofilm formation in *Klebsiella pneumoniae*. Pathogens (basel, Switzerland) 8:277. https://doi.org/10.3390/pathogens8040277

Diaz Iglesias Y, Van Bambeke F (2020) Activity of antibiotics against *Pseudomonas aeruginosa* in an *in vitro* model of biofilms in the context of cystic fibrosis: influence of the culture medium. Antimicrob Agents Chemother 64:e02204-e2219. https://doi.org/10.1128/AAC.02204-19

Feldman C, Kassel M, Cantrell J, Kaka S, Morar R, Goolam Mahomed A, Philips JI (1999) The presence and sequence of endotracheal tube colonization in patients undergoing mechanical ventilation. Eur Respir J 13:546–551. https://doi.org/10.1183/09031936.99.13354699

Ferrer MCC, Hickok NJ, Eckmann DM, Composto RJ (2012) Antibacterial biomimetic hybrid films. Soft Matter 8:2423–2431. https://doi.org/10.1039/C2SM06969E

Fox C, Daly M, Bellis TJJoVE, Care C, (2021) Identification of ventilator-associated pneumonia in dogs and evaluation of empiric antimicrobial therapy: 13 cases (2012–2016). J Vet Emerg Crit Care 31:66–73. https://doi.org/10.1111/vec.13032

Giacobbe DR, Battaglini D, Enrile EM, Dentone C, Vena A, Robba C, Ball L, Bartoletti M, Coloretti I, Di Bella S, Di Biagio A, Brunetti I, Mikulska M, Carannante N, De Maria A, Magnasco L, Maraolo AE, Mirabella M, Montrucchio G, Patroniti N, Taramasso L, Tiseo G, Fornaro G, Fraganza F, Monastra L, Roman-Pognuz E, Paluzzano G, Fiorentino G, Corcione A, Bussini L, Pascale R, Corcione S, Tonetti T, Rinaldi M, Falcone M, Biagioni E, Ranieri VM, Giannella M, De Rosa FG, Girardis M, Menichetti F, Viale P, Pelosi P, Bassetti M (2021) Incidence and prognosis of ventilator-associated pneumonia in critically ill patients with COVID-19: a multicenter study. J Clin Med 10:555. https://doi.org/10.3390/jcm10040555

Gorman S, Adair C, O'Neill F, Goldsmith C, Webb H (1993) Influence of selective decontamination of the digestive tract on microbial biofilm formation on endotracheal tubes from artificially ventilated patients. Eur J Clin Microbiol Infect Dis 12:9–17. https://doi.org/10.1007/bf01997050

Gurunathan S, Han JW, Kwon DN, Kim JH (2014) Enhanced antibacterial and anti-biofilm activities of silver nanoparticles against Gram-negative and Gram-positive bacteria. Nanoscale Res Lett 9:373. https://doi.org/10.1186/1556-276x-9-373

Hoffman CL, Lalsiamthara J, Aballay A (2020) Host mucin is exploited by *Pseudomonas aeruginosa* to provide monosaccharides required for a successful infection. mBio 11:e00060–20 https://doi.org/10.1128/mBio.00060-20

Ippolito M, Misseri G, Catalisano G, Marino C, Ingoglia G, Alessi M, Consiglio E, Gregoretti C, Giarratano A, Cortegiani A (2021) Ventilator-associated pneumonia in patients with COVID-19: a systematic review and meta-analysis. Antibiotics (basel, Switzerland) 10:545. https://doi.org/10.3390/antibiotics10050545

Kollef MH, Afessa B, Anzueto A, Veremakis C, Kerr KM, Margolis BD, Craven DE, Roberts PR, Arroliga AC, Hubmayr RD, Restrepo MI, Auger WR, Schinner R (2008) Silver-coated endotracheal tubes and incidence of ventilator-associated pneumonia: the NASCENT randomized trial. JAMA 300:805–813. https://doi.org/10.1001/jama.300.7.805

Lethongkam S, Daengngam C, Tansakul C, Siri R, Chumpraman A, Phengmak M, Voravuthikunchai SP (2020) Prolonged inhibitory effects against planktonic growth, adherence, and biofilm formation of pathogens causing ventilator-associated pneumonia using a novel polyamide/silver nanoparticle composite-coated endotracheal tube. Biofouling 36:292–307. https://doi.org/10.1080/08927014.2020.1759041

LewisOscar F, Nithya C, Vismaya S, Arunkumar M, Pugazhendhi A, Nguyen-Tri P, Alharbi SA, Alharbi NS, Thajuddin N (2021) *In vitro* analysis of green fabricated silver nanoparticles (AgNPs) against *Pseudomonas aeruginosa* PA14 biofilm formation, their application on urinary catheter. Prog Org Coat 151:106058. https://doi.org/10.1016/j.porgcoat.2020.106058

Lisboa T, Diaz E, Sa-Borges M, Socias A, Sole-Violan J, Rodríguez A, Rello J (2008) The ventilator-associated pneumonia PIRO score: a tool for predicting ICU mortality and health-care resources use in ventilator-associated pneumonia. Chest 134:1208–1216. https://doi.org/10.1378/chest.08-1106

Mas-Moruno C, Su B, Dalby MJ (2019) Multifunctional coatings and nanotopographies: toward cell instructive and antibacterial implants. Adv Healthc Mater 8:e1801103. https://doi.org/10.1002/adhm.201801103

Mizgerd JP, Skerrett SJ (2008) Animal models of human pneumonia. Am J Physiol Lung Cell Mol Physiol 294:L387–L398. https://doi.org/10.1152/ajplung.00330.2007

Muller L, Murgia X, Siebenburger L, Borger C, Schwarzkopf K, Sewald K, Haussler S, Braun A, Lehr CM, Hittinger M, Wronski S (2018) Human airway mucus alters susceptibility of *Pseudomonas aeruginosa* biofilms to tobramycin, but not colistin. Antimicrob Chemother 73:2762–2769. https://doi.org/10.1093/jac/dky241

Nwabor OF, Sudarshan S, Paosen S, Vongkamjan K, Voravuthikunchai SP (2020) Enhancing food shelf life with polyvinyl alcohol-chitosan polymer nanocomposite films from bioactive Eucalyptus leaf extracts. Food Biosci 36:100609. https://doi.org/10.1016/j.fbio.2020.100609

Oikkonen M, Aromaa U (1997) Leakage of fluid around low-pressure tracheal tube cuffs. Anaesthesia 52:567–569. https://doi.org/10.1111/j.1365-2044.1997.149-az0153.x

Olson ME, Harmon BG, Kollef MH (2002) Silver-coated endotracheal tubes associated with reduced bacterial burden in the lungs of mechanically ventilated dogs. Chest 121:863–870. https://doi.org/10.1378/chest.121.3.863

Paosen S, Jindapol S, Soontarach R, Voravuthikunchai SP (2019) *Eucalyptus citriodora* leaf extract-mediated biosynthesis of silver nanoparticles: broad antimicrobial spectrum and mechanisms of

action against hospital-acquired pathogens. APMIS 127:764–778. https://doi.org/10.1111/apm.12993

Paosen S, Lethongkam S, Wunnoo S, Lehman N, Kalkornsurapranee E, Septama AW, Voravuthikunchai SP (2021) Prevention of nosocomial transmission and biofilm formation on novel biocompatible antimicrobial gloves impregnated with biosynthesized silver nanoparticles synthesized using *Eucalyptus citriodora* leaf extract. Biotechnol J 16:e2100030. https://doi.org/10.1002/biot.202100030

Rehan M, Nada AA, Khattab TA, Abdelwahed NA, Abou El-Kheir AA (2020) Development of multifunctional polyacrylonitrile/silver nanocomposite films: antimicrobial activity, catalytic activity, electrical conductivity, UV protection and SERS-active sensor. J Mater Res Technol 9:9380–9394. https://doi.org/10.1016/j.jmrt.2020.05.079

Rello J, Afessa B, Anzueto A, Arroliga AC, Olson ME, Restrepo MI, Talsma SS, Bracken RL, Kollef MH (2010) Activity of a silver-coated endotracheal tube in preclinical models of ventilator-associated pneumonia and a study after extubation. Crit Care Med 38:1135–1140. https://doi.org/10.1097/CCM.0b013e3181cd12b8

Rivero PJ, Urrutia A, Goicoechea J, Zamarreño CR, Arregui FJ, Matías IR (2011) An antibacterial coating based on a polymer/sol-gel hybrid matrix loaded with silver nanoparticles. Nanoscale Res Lett 6:1–7. https://dx.doi.org/10.1186%2F1556-276X-6-305

Roosjen A, Norde W, van der Mei HC, Busscher HJ (2006) The use of positively charged or low surface free energy coatings versus polymer brushes in controlling biofilm formation. Prog Colloid Polym Sci 132:138–144. https://doi.org/10.1007/2882_026

Rubin BK, Ramirez O, Zayas JG, Finegan B, King M (1990) Collection and analysis of respiratory mucus from subjects without lung disease. Am Rev Respir Dis 141:1040–1043. https://doi.org/10.1164/ajrccm/141.4_pt_1.1040

Rutter CR, Rozanski EA, Sharp CR, Powell LL, Kent MJ (2011) Outcome and medical management in dogs with lower motor neuron disease undergoing mechanical ventilation: 14 cases (2003–2009). J Vet Emerg Crit Care 21:531–541. https://doi.org/10.1111/j.1476-4431.2011.00669.x

Rutter PR, Vincent B (1980) The adhesion of microorganisms to surfaces: physico-chemical aspects. In: Berkeley RCW, Lynch JM, Melling J, Rutter PR, Vincent B (eds) Microbial Adhesion to Surfaces. Ellis Horwood, Chichester, pp 79–92

Samad T, Co JY, Witten J, Ribbeck K (2019) Mucus and mucin environments reduce the efficacy of polymyxin and fluoroquinolone antibiotics against *Pseudomonas aeruginosa*. ACS Biomater Sci Eng 5:1189–1194. https://doi.org/10.1021/acsbiomaterials.8b01054

Scheuerman TR, Camper AK, Hamilton MA (1998) Effects of substratum topography on bacterial adhesion. J Colloid Interface Sci 208:23–33. https://doi.org/10.1006/jcis.1998.5717

Seitz AP, Schumacher F, Baker J, Soddemann M, Wilker B, Caldwell CC, Gobble RM, Kamler M, Becker KA, Beck S, Kleuser B, Edwards MJ, Gulbins E (2019) Sphingosine-coating of plastic surfaces prevents ventilator-associated pneumonia. J Mol Med (berl) 97:1195–1211. https://doi.org/10.1007/s00109-019-01800-1

Singh AV, Vyas V, Patil R, Sharma V, Scopelliti PE, Bongiorno G, Podestà A, Lenardi C, Gade WN, Milani P (2011) Quantitative characterization of the influence of the nanoscale morphology of nanostructured surfaces on bacterial adhesion and biofilm formation. PLoS ONE 6:e25029. https://doi.org/10.1371/journal.pone.0025029

Soares RM, de ASRM, Alviano DS, Angluster J, Alviano CS, Travassos LR, (2000) Identification of sialic acids on the cell surface of *Candida albicans*. Biochim Biophys Acta 1474:262–268. https://doi.org/10.1016/s0304-4165(00)00003-9

Su C, Ye Y, Qiu H, Zhu Y (2021) Solvent-free fabrication of self-regenerating antibacterial surfaces resisting biofilm formation. ACS Appl Mater Interfaces 13:10553–10563. https://doi.org/10.1021/acsami.0c20033

Syukri DM, Nwabor OF, Singh S, Voravuthikunchai SP (2021) Antibacterial functionalization of nylon monofilament surgical sutures through *in situ* deposition of biogenic silver nanoparticles. Surf Coat Technol 413:127090. https://doi.org/10.1016/j.surfcoat.2021.127090

Triebel C, Vasylyev S, Damm C, Stara H, Özpınar C, Hausmann S, Peukert W, Münstedt H (2011) Polyurethane/silver-nanocomposites with enhanced silver ion release using multifunctional invertible polyesters. J Mater Chem 21:4377–4383. https://doi.org/10.1039/C0JM03487H

Wang T-J, Chang H-W, Chen J-S, Chiang H-P (2019) Nanotip-assisted photoreduction of silver nanostructures on chemically patterned ferroelectric crystals for surface enhanced Raman scattering. Sci Rep 9:1–10. https://doi.org/10.1038/s41598-019-47523-8

Wintachai P, Paosen S, Yupanqui CT, Voravuthikunchai SP (2019) Silver nanoparticles synthesized with *Eucalyptus critriodora* ethanol leaf extract stimulate antibacterial activity against clinically multidrug-resistant *Acinetobacter baumannii* isolated from pneumonia patients. Microb Pathog 126:245–257. https://doi.org/10.1016/j.micpath.2018.11.018

Wu S, Altenried S, Zogg A, Zuber F, Maniura-Weber K, Ren Q (2018) Role of the surface nanoscale roughness of stainless steel on bacterial adhesion and microcolony formation. ACS Omega 3:6456–6464. https://doi.org/10.1021/acsomega.8b00769

Wu Z, McGoogan JM (2020) Characteristics of and important lessons from the coronavirus disease 2019 (COVID-19) outbreak in China: summary of a report of 72 314 cases from the Chinese Center for Disease Control and Prevention. JAMA 323:1239–1242. https://doi.org/10.1001/jama.2020.2648

Wunnoo S, Paosen S, Lethongkam S, Sukkurd R, Waen-ngoen T, Nuidate T, Phengmak M, Voravuthikunchai SP (2021) Biologically rapid synthesized silver nanoparticles from aqueous *Eucalyptus camaldulensis* leaf extract: effects on hyphal growth, hydrolytic enzymes, and biofilm formation in *Candida albicans*. Biotechnol Bioeng 118:1597–1611. https://doi.org/10.1002/bit.27675

Yu P, Wang C, Zhou J, Jiang L, Xue J, Li W (2016) Influence of surface properties on adhesion forces and attachment of *Streptococcus mutans* to zirconia in vitro. Biomed Res Int 2016:8901253. https://doi.org/10.1155/2016/8901253

Zhang S, Liang X, Gadd GM, Zhao Q (2019) Superhydrophobic coatings for urinary catheters to delay bacterial biofilm formation and catheter-associated urinary tract infection. ACS Appl Bio Mater 3:282–291. https://doi.org/10.1021/acsabm.9b00814

Zhang S, Liang X, Gadd GM, Zhao Q (2021) A sol–gel based silver nanoparticle/polytetrafluorethylene (AgNP/PTFE) coating with enhanced antibacterial and anti-corrosive properties. Appl Surf Sci 535:147675. https://doi.org/10.1016/j.apsusc.2020.147675

Zur KB, Mandell DL, Gordon RE, Holzman I, Rothschild MA (2004) Electron microscopic analysis of biofilm on endotracheal tubes removed from intubated neonates. Otolaryngol Head Neck Surg 130:407–414. https://doi.org/10.1016/j.otohns.2004.01.006